Traveling waves in ferroelectric smectic-*C* liquid crystals

I. W. Stewart
Department of Mathematics, University of Strathclyde, Livingstone Tower, 26 Richmond Street, Glasgow G1 1XH, United Kingdom

E. Momoniat
Centre for Differential Equations, Continuum Mechanics and Applications, School of Computational and Applied Mathematics, University of the Witwatersrand, Private Bag 3, Wits 2050, South Africa

(Received 22 January 2004; revised manuscript received 18 March 2004; published 22 June 2004)

This article investigates, by means of Lie point symmetries, traveling wave solutions to a dynamic equation that frequently arises in the theory of ferroelectric smectic-*C* liquid crystals under the influence of an electric field. The equation considered has three sinusoidal nonlinearities and possible time-dependent solutions are discussed in the context of minima and maxima of the electric energy density for these liquid crystals: solutions travel between such constant equilibrium states. Implicit solutions to an approximation of the governing dynamic equation are determined. Nondimensional control parameters that characterize changes in the availability of equilibrium states as the magnitude of the field increases are also identified.

DOI: 10.1103/PhysRevE.69.061714 PACS number(s): 61.30.Cz

I. INTRODUCTION

Traveling wave phenomena and "solitonlike" behavior arise frequently in the liquid crystal literature. There has been much interest recently in the construction of traveling wave solutions to problems that arise in the switching processes of smectic-*C* (Sm*C*) and chiral ferroelectric smectic-*C* (Sm*C**) liquid crystals, especially those problems related to high speed flat panel display technology. A general introduction to these topics may be found in the books by Lam and Prost [1], de Gennes and Prost [2], Lagerwall [3] and Stewart [4]. The possibility of exploiting solitonlike effects in the switching dynamics of Sm*C** liquid crystals was first raised by Clark and Lagerwall [5] and has been extensively studied by many other authors in relation to applications: some relevant references will be mentioned below at appropriate stages. It is the aim of this article to present some traveling wave solutions to a dynamic equation [Eq. (2.11)] which has been employed in the literature for describing the behavior of switching in Sm*C** liquid crystals [6–8] and to give a general discussion of the relevant electric energy density and its maxima and minima. A description of this governing equation and a brief study of the electric energy are given in Secs. II and III, respectively. Section IV investigates solutions via Lie point symmetries and presents some traveling wave solutions in implicit form. The key equation developed below incorporates, as a special case, a well-known dynamic equation which possesses an exact traveling wave solution; this special solution [given by Eq. (2.13), or, equivalently, by Eq. (4.14) below] has previously been studied extensively (see, for example, [9–14]) and will be derived in a novel way via Lie point symmetries in Sec. IV B. It will form the starting point for the derivation of traveling wave solutions to an approximation of the more general equation to be discussed in Secs. IV C and IV D. Implicit traveling wave solutions are determined in Sec. IV C for such an approximation to the general equation and two examples are calculated and presented in Sec. IV D. The article closes with a short discussion in Sec. V.

II. DESCRIPTION OF THE PROBLEM

Liquid crystals are anisotropic fluids consisting of elongated molecules for which the long molecular axes locally adopt one common direction in space described by the unit vector **n**, called the director. It is assumed that **n** and −**n** are physically indistinguishable, which leads to certain invariance properties in the energetic description of liquid crystals. Sm*C* liquid crystals are layered structures in which the director **n** is, in the isothermal situation, tilted at a constant angle θ to the normal of equally spaced layers as shown in Fig. 1(a), the unit normal to the smectic layers being denoted by the vector **a**. Following de Gennes and Prost [2], it is common practice to introduce the unit orthogonal projection **c** of **n** onto the smectic planes; **c** is always perpendicular to the smectic layer normal. The orientation of **n** can be deduced from the orientation of **a** and **c**, as can be seen from the description provided in Fig. 1(b) where it is evident that

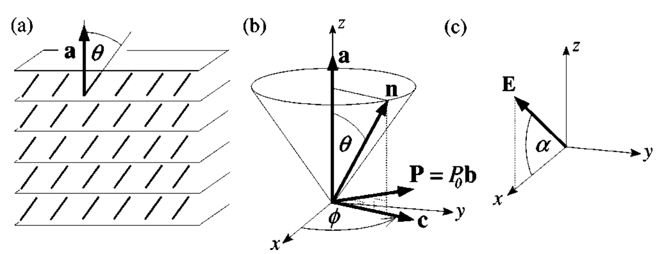

FIG. 1. (a) Sm*C** liquid crystals form parallel layers with the director tilted at a constant angle θ to the unit layer normal **a**. (b) The mathematical description of the orientation of the director **n** is accomplished by introducing the unit orthogonal projection **c** of **n** onto the local smectic planes. The orientation angle ϕ of **c** allows a complete description of the director alignment via the relation (2.1). The spontaneous polarization, which is characteristic of Sm*C**, is denoted by $P_0\mathbf{b}$ where $\mathbf{b}=\mathbf{a}\times\mathbf{c}$. (c) An electric field **E** is applied at a constant angle $\alpha \geqslant 0$ relative to the smectic layers as shown.

1539-3755/2004/69(6)/061714(9)/$22.50 ©2004 The American Physical Society

$$\mathbf{n} = \mathbf{a}\cos\theta + \mathbf{c}\sin\theta. \tag{2.1}$$

When **a** is fixed, as it will be here, then knowledge of the orientation angle ϕ of the vector **c**, as depicted in Fig. 1(b), leads to a complete understanding of the orientation of **n** through the above relation. SmC* liquid crystals have, in addition to the aforementioned properties, an inherent spontaneous polarization **P** satisfying, according to the convention for positive polarization, $\mathbf{P}=P_0\mathbf{b}$ where $P_0>0$ is its magnitude and **b** is defined to be the unit vector $\mathbf{a}\times\mathbf{c}$. A description for positive spontaneous polarisation is shown in Fig. 1(b). The sign of **P** may actually be positive or negative and depends on the particular material; this leads to the convention of calling **P** positive if $\mathbf{P}=P_0\mathbf{b}$ and negative if $\mathbf{P}=-P_0\mathbf{b}$. We shall be able to discuss both cases. The equation discussed below can be derived from the nonlinear dynamic continuum theory for SmC liquid crystals introduced by Leslie *et al.* [15,16]. This theory can be extended to include SmC* liquid crystals by incorporating a suitable elastic energy density, as discussed by Carlsson *et al.* [17]. A summary of this continuum theory for SmC and SmC* liquid crystals may be found in the book by Stewart [4] or the review article by Leslie [18], while more detailed general properties of smectic liquid crystals may be found in [2,3].

Consider a sample of SmC* liquid crystal in the planar layer arrangement of Fig. 1(a) under the application of an externally applied electric field **E** as shown in Fig. 1(c). The electric field is tilted by a fixed constant angle α with respect to the plane of the layers and is oriented in the xz plane. From Figs. 1(b) and 1(c) it follows that we can set

$$\mathbf{a} = (0,0,1), \tag{2.2}$$

$$\mathbf{c} = (\cos\phi(x,t), \sin\phi(x,t), 0), \tag{2.3}$$

$$\mathbf{b} = (-\sin\phi(x,t), \cos\phi(x,t), 0), \tag{2.4}$$

$$\mathbf{P} = P_0\mathbf{b}, \tag{2.5}$$

$$\mathbf{E} = E(\cos\alpha, 0, \sin\alpha), \tag{2.6}$$

where the dependence of the orientation angle ϕ upon x and t only is supposed and E is the magnitude of the electric field. These vectors satisfy the four constraints of smectic-C continuum theory [15], namely,

$$\mathbf{a}\cdot\mathbf{a} = 1,\ \mathbf{c}\cdot\mathbf{c} = 1,\ \mathbf{a}\cdot\mathbf{c} = 0,\ \nabla\times\mathbf{a} = \mathbf{0}. \tag{2.7}$$

The total electric energy density is given by [2–4]

$$w_{elec} = -\mathbf{P}\cdot\mathbf{E} - \frac{1}{2}\epsilon_0\epsilon_a(\mathbf{n}\cdot\mathbf{E})^2, \tag{2.8}$$

where $\epsilon_0 = 8.854\times10^{-12}$ F m^{-1} is the permittivity of free space and ϵ_a is the (unitless) dielectric anisotropy, which can be positive or negative. Substituting the appropriate quantities from Eq. (2.1) to Eq. (2.6) into w_{elec} shows that we have

$$w_{elec} = P_0E\cos\alpha\sin\phi - \frac{1}{2}\epsilon_0\epsilon_a E^2(\sin\alpha\cos\theta + \cos\alpha\sin\theta\cos\phi)^2. \tag{2.9}$$

When the influence of flow is neglected and the smectic elastic constants B_1 and B_2 are set equal to $B>0$, the dynamic equation for the orientation angle ϕ is given by

$$2\lambda_5\frac{\partial\phi}{\partial t} = B\frac{\partial^2\phi}{\partial x^2} - \frac{\partial w_{elec}}{\partial\phi}, \tag{2.10}$$

which leads to the governing equation

$$2\lambda_5\frac{\partial\phi}{\partial t} = B\frac{\partial^2\phi}{\partial x^2} - P_0E\cos\alpha\cos\phi - \epsilon_0\epsilon_a E^2\cos\alpha\sin\alpha\cos\theta\sin\theta\sin\phi - \epsilon_0\epsilon_a E^2\cos^2\alpha\sin^2\theta\sin\phi\cos\phi. \tag{2.11}$$

A rigorous derivation of this equation may be obtained by calculations similar to those presented elsewhere [4,19]. The coefficient $\lambda_5>0$ is a rotational viscosity related to the rotation of the director **n** around a fictitious cone as shown in Fig. 1(b). We are concerned with finding possible traveling wave solutions to this equation. The general form of this equation with sinusoidal nonlinearities in ϕ appears in various models: only the constant coefficients change in accordance with the corresponding model [6–8]. The general case will be considered below in Sec. IV.

A. special case

When $\alpha=0$, Eq. (2.11) reduces to

$$2\lambda_5\frac{\partial\phi}{\partial t} = B\frac{\partial^2\phi}{\partial x^2} - P_0E\cos\phi - \epsilon_0\epsilon_a E^2\sin^2\theta\sin\phi\cos\phi. \tag{2.12}$$

This special case arises when considering the switching of SmC* liquid crystals where ϕ will change from one constant state, say ϕ_1, to another, ϕ_2, as time progresses. There is a well-known traveling wave solution to Eq. (2.12) when $\epsilon_a<0$ which can be obtained from the solution presented in Refs. [4,9–11,13,19] (for example, by redefining the constant coefficients and making the substitution $\phi\mapsto\pi/2-\phi$). It is given explicitly by

$$\phi(x,t) = \frac{\pi}{2} - 2\tan^{-1}\left[\exp\left\{\sqrt{\frac{\beta}{B}}(x\pm \mathsf{v}t)\right\}\right], \tag{2.13}$$

where β and the wave speed v are defined by, respectively,

$$\beta = \epsilon_0|\epsilon_a|E^2\sin^2\theta,\quad \mathsf{v} = \frac{|P_0E|}{2\lambda_5}\sqrt{\frac{B}{\beta}}, \tag{2.14}$$

noting that $\epsilon_a=-|\epsilon_a|$ when $\epsilon_a<0$. In the solution (2.13), the plus sign is taken when $P_0E>0$ and the negative sign is taken when $P_0E<0$. Changing the sign of P_0E is equivalent to reversing the sign of the electric field. One observes that reversing the sign of the electric field then reverses the direction of the velocity of the traveling wave. Further, for this

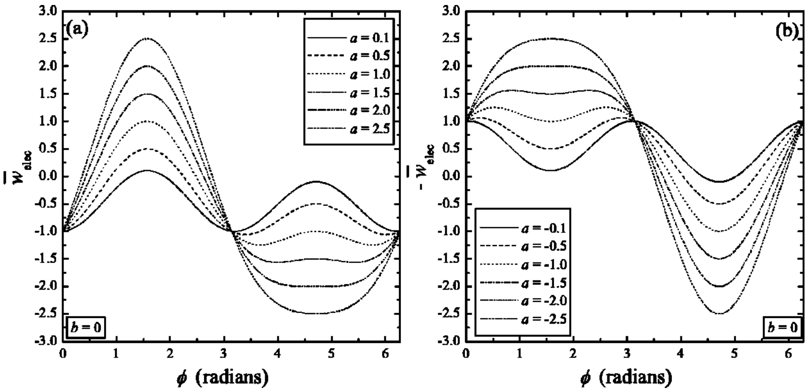

FIG. 2. Plots of (a) $\overline{w}_{elec}$ for $a>0$ and (b) $-\overline{w}_{elec}$ for $a<0$ (which then has the same sign as w_{elec}), defined in Eq. (3.4), as a function of ϕ when $b=0$ for various values of the dimensionless parameter a. Decreasing the magnitude of a corresponds to increasing the magnitude of the electric field **E**. The number of equilibria changes from two to four as the magnitude of a decreases through the critical value $|a_c^0|=2$, as discussed in the text.

solution, it is seen that for $P_0E>0$, $\phi\to+\pi/2$ as $t\to-\infty$ and $\phi\to-\pi/2$ as $t\to+\infty$. This represents a reorientation of **c** through π radians. The availability of these particular constant states between which the solution travels can be identified from a consideration of the electric energy density, as has been discussed by Stewart *et al.* [19] in the case of Sm*C* liquid crystals under the influence of a tilted electric field. In [19, Eq. (2,10)], the governing dynamic equation is identical in form to Eq. (2.11) if P_0 is set to zero and B is replaced by the elastic constant B_3. It is therefore worthwhile to investigate the features of the electric energy density which yield the electrical contributions to Eq. (2.11).

III. THE ELECTRIC ENERGY

To facilitate a qualitative discussion of this energy density and a simplification of the dynamic equation (2.11) in such a way that it can be related more easily to the general results already available in the literature, it proves convenient to introduce the dimensionless parameters

$$a = 2P_0(\epsilon_0\epsilon_a E\cos\alpha\sin^2\theta)^{-1}, \tag{3.1}$$

$$b = \tan\alpha\cot\theta. \tag{3.2}$$

We can then write the electric energy density (2.9) as

$$w_{elec} = \frac{1}{2}\epsilon_0\epsilon_0 E^2\cos^2\alpha\sin^2\theta\,\overline{w}_{elec}, \tag{3.3}$$

where the dimensionless quantity $\overline{w}_{elec}$ is defined by

$$\overline{w}_{elec} = a\sin\phi - (b+\cos\phi)^2. \tag{3.4}$$

Reversing the sign of the electric field is equivalent to changing the sign of a. Also, it is seen that changing the signs of ϵ_a and E simultaneously is equivalent to changing the sign of w_{elec} and therefore all possible situations can be classified qualitatively by considering $\overline{w}_{elec}$.

From physical considerations it is only necessary to consider $b\geq 0$ because it has been supposed that $0<\theta<\pi/2$ and $0\leq\alpha<\pi/2$. The parameter b is a measure of the tilt of the field, while a can take positive or negative values and is a measure of the ratio of the spontaneous polarization P_0 to the magnitude of the electric field **E**; $|a|$ decreases as $|E|$ increases. For the typical estimates

$$\epsilon_a = -2,\ \theta = 22°,\ \alpha = 5°,\ P_0 = 80\ \mu\text{C m}^{-2},\ E = 30\ \text{V}\ \mu\text{m}^{-1}, \tag{3.5}$$

we obtain the approximate values

$$a = -2.154,\ b = 0.217, \tag{3.6}$$

and so it is expected that in general $b<|a|$ for applied fields with a small tilt α, especially so for smaller magnitude fields where a is large. Clearly, b decreases to zero as α decreases to zero.

Figure 2 shows the main features of $\overline{w}_{elec}$ when $b=0$, which corresponds to the special case $\alpha=0$ discussed in Sec. II. The left and right graphs show the situation for $a>0$ and $a<0$, respectively; for $a<0$ we have plotted $-\overline{w}_{elec}$ so that w_{elec} has the same sign as the graphs shown in Fig. 2(b) [cf. Eq. (3.3)]. These graphs are 2π periodic. In both graphs it is evident that as $|a|$ decreases, the function $\overline{w}_{elec}$ changes from having one maximum and one minimum to having two maxima and two minima whenever $|a|$ is below some critical magnitude, that is, whenever $|E|$ is sufficiently large. When $b=0$ this critical value can be identified by differentiating $\overline{w}_{elec}$ and seeking the equilibrium points: it is straightforward to find that the critical value is given by $|a_c^0|=2$. Notice that in Fig. 2(a) the local maximum at $\phi=\pi/2$ remains a maximum as a $a>0$ decreases but that the local minimum at $\phi=\frac{3}{2}\pi$ becomes a local maximum as two other minima are introduced; for a given small fixed value of a, the energies of the two maxima always differ while the two minima have equal energy. There is an analogous situation for $a<0$ depicted in Fig. 2(b). These maxima and minima represent the equilibrium states for the electric energy density and traveling wave solutions are known to connect such states. For example, the solution (2.13) for $b=0$ connects the equilibria at $\phi=-\pi/2$ and $\phi=\pi/2$ and can be identified by considering Fig. 2.

The graphs in Fig. 3 show $\overline{w}_{elec}$ for $b=0.217$, motivated by the data which yield the results in Eq. (3.6). For large fixed values of $a>0$, only one maximum and one minimum in Fig. 3(a) appear, as before in Fig. 2(a). Further, as $a>0$ decreases in Fig. 3(a), the local minimum retains its character but occurs at an increasing value of ϕ, as shown. At the same time, another local minimum and a local maximum are introduced for sufficiently small a, but, unlike the case in Fig. 2(a), all the local minima and maxima have different

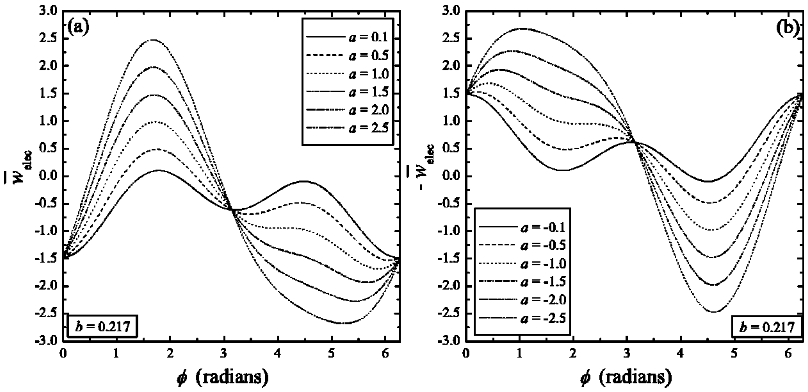

FIG. 3. (a) $\overline{w}_{elec}$ for $a>0$ and (b) $-\overline{w}_{elec}$ for $a<0$ for various values of a as a function of ϕ when $b=0.217$. These values are motivated by the example in Eqs. (3.5) and (3.6).

energies for a given fixed value of a. The analogous situation for $a<0$ is shown in Fig. 3(b) where, for the reason mentioned previously for Fig. 2(b), we have plotted $-\overline{w}_{elec}$ so that the graph has the same sign as w_{elec}. For a given value of b, it is evident therefore that there exists a critical value of a_c (generally found by examining the derivative of $\overline{w}_{elec}$ and obtaining the equilibrium points by numerical means for a given set of parameter values) which influences the occurrence of maxima and minima. In general, for $|a|>|a_c|$, $\overline{w}_{elec}$ defined by Eq. (3.4) only possesses two real equilibria, whereas for $|a|<|a_c|$ four real equilibria occur (all modulo 2π of course). Figure 4(a) demonstrates this situation for the typical parameter $b=0.217$, which arose earlier at Eq. (3.6). The value of a_c in this case can be identified as approximately 1.021. A comparison with Fig. 3(a) shows this to be the case: one local maximum and one local minimum occur for $a>a_c$ while two local minima and two local maxima are introduced for $a<a_c$. Figure 4(b) shows the dependence of a_c upon b; in particular, it demonstrates that there are only ever two equilibria for any $b\geqslant 0$ whenever $a\geqslant 2$ (recall that we earlier identified $a_c=2$ when $a>0$ and $b=0$). There are four equilibria for values of a and b corresponding to points below the given curve and two equilibria for points above it.

IV. SOLUTIONS VIA LIE POINT SYMMETRIES

We begin by transforming Eq. (2.11) into a nondimensional form in order to relate the general equation to results that are already available in the literature. An application of Lie point symmetries will then be made for the special case when the tilt of the electric field α is zero, equivalent to $b=0$. This method will, first, reproduce the nondimensional version of the solution (2.13) to Eq. (2.12) and, secondly, will enable us to generate solutions to Eq. (2.11) for small $b\neq 0$ by considering the general equation (4.4) below as a perturbation of Eq. (4.5).

A. The nondimensional equation

For simplicity, it will be assumed that $\epsilon_a<0$, which is known to be the case for many SmC* liquid crystals. We can then introduce the scaled variables

$$T=\frac{1}{4}t(2\lambda_5)^{-1}\epsilon_0|\epsilon_a|E^2\cos^2\alpha\sin^2\theta,$$
$$X=\frac{1}{2}xB^{-1/2}(\epsilon_0|\epsilon_a|E^2\cos^2\alpha\sin^2\theta)^{1/2}. \tag{4.1}$$

Noting, as above, that $\epsilon_a=-|\epsilon_a|$ for $\epsilon_a<0$, Eq. (2.11) can now be nondimensionalized to

$$\phi_T=\phi_{XX}+2a\cos\phi+4b\sin\phi+2\sin(2\phi), \tag{4.2}$$

where subscripts denote partial differentiation with respect to the indicated variables. Making the further transformation

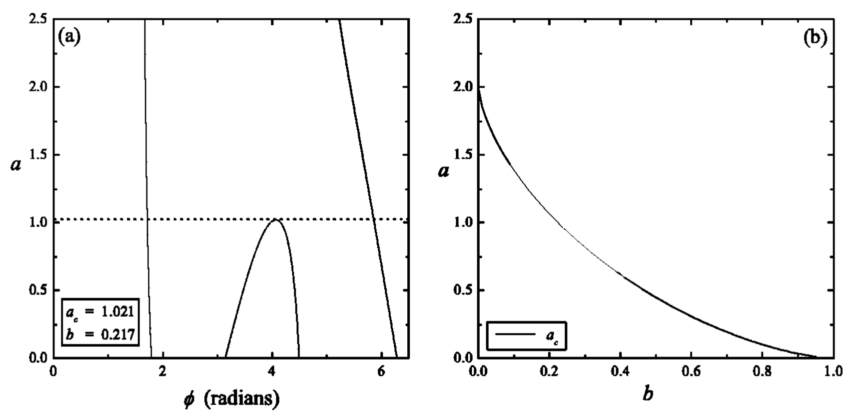

FIG. 4. (a) The equilibria of $\overline{w}_{elec}$ defined by Eq. (3.4) as a decreases to zero for the particular value of $b=0.217$. Similar graphs arise for other values of b between 0 and 1. The dotted line represents a critical value of a, given approximately by $a_c=1.021$. For $a>a_c$ only two real equilibria occur, while for $a<a_c$ four real equilibria become available. A direct comparison with the results in Fig. 3(a) is possible. (b) A general plot of how a_c depends upon b. $\overline{w}_{elec}$ has four equilibria for values of a and b corresponding to points below the given curve and two equilibria for points above it.

$$u(X,T) = 2\phi(X,T) - \pi, \tag{4.3}$$

finally delivers the nondimensional equation in a standard form as (cf. [13])

$$u_T = u_{XX} - 4a \sin\left(\frac{u}{2}\right) - 4 \sin u + 8b \cos\left(\frac{u}{2}\right). \tag{4.4}$$

B. Lie point symmetries

By considering Lie point symmetries of the partial differential equation

$$u_T = u_{XX} - 4a \sin\left(\frac{u}{2}\right) - 4 \sin u, \tag{4.5}$$

which is the special case discussed previously when $b=0$, it can be shown (see Appendix) that Eq. (4.5) admits traveling wave solutions of the form

$$u(X,T) = F(p), \; p = X + vT. \tag{4.6}$$

Substituting Eq. (4.6) into Eq. (4.5) we obtain the second-order ordinary differential equation

$$4\left[a \sin\left(\frac{F}{2}\right) + \sin(F)\right] + v\frac{dF}{dp} - \frac{d^2F}{dp^2} = 0. \tag{4.7}$$

Equation (4.7) admits a Lie point symmetry

$$Y = \partial_p. \tag{4.8}$$

Therefore we can make the substitutions

$$F'(p) = K(F), \; F''(p) = K\frac{dK}{dF}. \tag{4.9}$$

The second-order ordinary differential equation (4.7) reduces to the first-order ordinary differential equation

$$4\left[a \sin\left(\frac{F}{2}\right) + \sin(F)\right] + K\left(v - \frac{dK}{dF}\right) = 0. \tag{4.10}$$

Equation (4.10) is an Abel equation of the second kind. From results contained in Polyanin and Zaitsev [20], Eq. (4.10) admits a particular solution of the form

$$K(F) = \mp 4 \sin\left(\frac{F}{2}\right), \; v = \pm a. \tag{4.11}$$

Therefore, we can determine $F(p)$ by solving the first-order ordinary differential equation

$$\frac{dF}{dp} \pm 4 \sin\left(\frac{F}{2}\right) = 0, \; v = \pm a. \tag{4.12}$$

This ordinary differential equation has a solution

$$F(p) = 4 \arctan\{\exp[\mp 2(c + p)]\}, \; v = \pm a, \tag{4.13}$$

where c is a constant of integration. The solution (4.13) is widely known and has been obtained by various other methods, as has been discussed by, among others, Schiller *et al.* [9], Cladis and van Saarloos [10] and Maclennan *et al.* [11]. A Painlevé analysis by Stewart [13] also recovered this solution as a special case in a quite general context. Equation (4.13) can be rewritten in the original variables as

$$u(X,T) = 4 \arctan\{\exp[\mp 2(X + vT + c)]\}, \; v = \pm a. \tag{4.14}$$

1. Remark

Notice that $\pm u(X,T)$ are solutions to Eq. (4.5) for whichever value of v is adopted and that, by Eqs. (2.14) (first equation), (3.1) and (4.1), when $\epsilon_a < 0$ we have

$$2(X - aT) = \sqrt{\frac{\beta}{B}}\left(x + \frac{P_0 E}{2\lambda_5}\sqrt{\frac{B}{\beta}}t\right). \tag{4.15}$$

The explicit solution (2.13) to Eq. (2.12) can then be recovered from the result in Eq. (4.14) by setting $c=0$, $v=-a$ and considering the solution

$$u = -4 \arctan\{\exp[2(X - aT)]\}, \tag{4.16}$$

under the transformation (4.3). It is clear in this case that $u \to 0$ as $X \to -\infty$ and $u \to -2\pi$ as $X \to \infty$; this corresponds to the solution ϕ in Eq. (2.13) traveling between the equilibrium states $\pi/2$ and $-\pi/2$, as mentioned towards the end of Sec. II.

C. The perturbed equation

Given the form of b defined by Eq. (3.2), and that it is generally expected to be much smaller than a, it is natural to search for possible traveling wave solutions to Eq. (4.4) when $b \ll 1$. This can be accomplished by considering a perturbation of Eq. (4.5) of the form

$$u_T = u_{XX} - 4a \sin\left(\frac{u}{2}\right) - 4 \sin u + \epsilon \cos\left(\frac{u}{2}\right), \; \epsilon \ll 1, \tag{4.17}$$

where we have set $8b \equiv \epsilon$ for notational convenience. We look for traveling wave solutions of the form (4.6) admitted by Eq. (4.17). Substituting Eq. (4.6) into Eq. (4.17) we obtain

$$-\epsilon \cos\left(\frac{F}{2}\right) + 4a \sin\left(\frac{F}{2}\right) + 4 \sin(F) + v\frac{dF}{dp} - \frac{d^2F}{dp^2} = 0. \tag{4.18}$$

Equation (4.18) admits the Lie point symmetry generator (4.8). Hence we can make the substitutions (4.9) to obtain

$$-\epsilon \cos\left(\frac{F}{2}\right) + 4\left[a \sin\left(\frac{F}{2}\right) + \sin(F)\right] + K\left(v - \frac{dK}{dF}\right) = 0. \tag{4.19}$$

Equation (4.19) is again an Abel equation of the second kind. We look for solutions of the form

$$K(F) = K_0(F) + \epsilon K_1(F). \tag{4.20}$$

Substituting Eq. (4.20) into Eq. (4.19) and separating by coefficients of ϵ we obtain the system

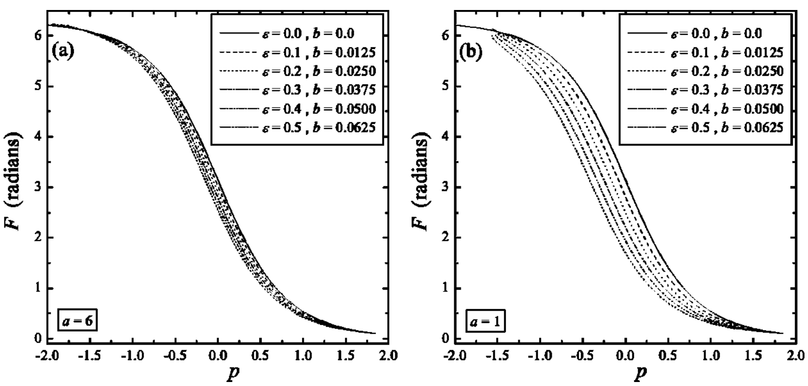

FIG. 5. Examples of approximate solutions to Eq. (4.17) for the indicated values of $\epsilon \equiv 8b$. These special cases arise from the general solution (4.29) when $v=+a$ with $c_1=0$. (a) The solution for $a=6$ in Eq. (4.30), which corresponds to a "low field" regime (a is greater than the maximum possible a_c for all $b \geqslant 0$) and (b) the case for $a=1$ in Eq. (4.31) for a "high field" regime where a and the values of b always lie below the curve a_c shown in Fig. 4(b).

$$4\left[a\sin\left(\frac{F}{2}\right)+\sin(F)\right]+K_0(F)\left(v-\frac{dK_0}{dF}\right)=0, \tag{4.21}$$

$$-\cos\left(\frac{F}{2}\right)+K_1\left(v-\frac{dK_0}{dF}\right)-K_0\frac{dK_1}{dF}=0. \tag{4.22}$$

From Eq. (4.11) we have that Eq. (4.21) admits the solution

$$K_0(F)=\mp 4\sin\left(\frac{F}{2}\right),\ v=\pm a. \tag{4.23}$$

Substituting Eq. (4.23) into Eq. (4.22) we obtain a first-order ordinary differential equation for $K_1(F)$, namely,

$$\pm 4\sin\left(\frac{F}{2}\right)\frac{dK_1}{dF}\pm\left[a+2\cos\left(\frac{F}{2}\right)\right]K_1-\cos\left(\frac{F}{2}\right)=0. \tag{4.24}$$

We can solve Eq. (4.24) in terms of an integrating factor and obtain

$$K_1(F)=\frac{1}{2}\left[\cos\left(\frac{F}{4}\right)\right]^{-1+a/2}\left[\sin\left(\frac{F}{4}\right)\right]^{-1-a/2}\times\left[c_0\pm\frac{1}{4}\int^F\left[\tan\left(\frac{s}{4}\right)\right]^{a/2}\cos\left(\frac{s}{2}\right)ds\right], \tag{4.25}$$

where c_0 is an integration constant. From Eqs. (4.9) and (4.20), to determine $F(p)$ we must finally solve

$$\frac{dF}{dp}=K_0(F)+\epsilon K_1(F). \tag{4.26}$$

Equation (4.26) simplifies to

$$\int\frac{dF}{K_0(F)+\epsilon K_1(F)}=\int dp. \tag{4.27}$$

Since $\epsilon \ll 1$, we can approximate the result (4.27) to

$$\int\frac{dF}{K_0(F)}-\epsilon\int\frac{K_1(F)}{K_0(F)^2}dF=\int dp. \tag{4.28}$$

For $v=\pm a$ we then have the corresponding implicit solutions for F given by

$$\mp\frac{1}{2}\ln\left[\tan\left(\frac{F}{4}\right)\right]-\frac{\epsilon}{128}\int^F\left[\cos\left(\frac{r}{4}\right)\right]^{-3+a/2}\left[\sin\left(\frac{r}{4}\right)\right]^{-3-a/2}\times\left[c_0\pm\frac{1}{4}\int^r\left[\tan\left(\frac{s}{4}\right)\right]^{a/2}\cos\left(\frac{s}{2}\right)ds\right]dr=p+c_1, \tag{4.29}$$

where c_1 is a constant of integration. In conjunction with Eq. (4.6), Eq. (4.29) represents an implicit solution for $u(X,T)$. Notice that this solution reduces to that stated in Eq. (4.13) when $\epsilon=0$. Further, the logarithmic term in the solution (4.29) will diverge more slowly than the contribution that involves ϵ as F approaches 2π; the approximate solution therefore becomes less accurate as a suitable model near the $F=2\pi$ regime; this behavior is apparent in the examples shown in Fig. 5.

D. Examples

To demonstrate some qualitative solutions, we can specialize to the case of $v=+a$ with $a>0$ and consider the solution (4.29) for some small values of $8b\equiv\epsilon>0$. Recall that for $a>2$ [cf. Fig. 4(b)] there are only ever two real equilibria for $\overline{w}_{elec}$. To ease calculations, we choose to look at the cases $a=6$ and $a=1$, set $c_0=0$ and put the lower and upper limits of the integral with respect to s appearing in Eq. (4.29) to 0 and r respectively; this integral is then always finite for $a>0$. For simplicity, the arbitrary constant c_1 can be chosen as zero. The choices for ϵ used in the plots of solutions in Fig. 5 have some physical relevance: for example, for a typical smectic cone angle of 22°, b varying from 0 to 0.0625 corresponds, via Eq. (3.2), to the tilt of the electric field varying from zero to around 14.3°. For values of $b>1$ the perturbed solution, despite being available, can be considered as no longer ideal for gaining insight into the behavior of the problem because Eq. (4.29) has been constructed under the assumption that $\epsilon\ll 1$.

1. Example 1: a=6

The solution when $a=6$ is obtained from Eq. (4.29) as

$$-\frac{1}{2}\ln\left[\tan\left(\frac{F}{4}\right)\right] - \frac{\epsilon}{512}\int^{F}\left[\sin\left(\frac{r}{4}\right)\right]^{-6}\int_0^r\left[\tan\left(\frac{s}{4}\right)\right]^{3}\cos\left(\frac{s}{2}\right)dsdr = p, \tag{4.30}$$

recalling that $p\equiv X+aT$ here. The resulting solutions are shown in Fig. 5(a) for a selection of positive values for ϵ, with $\epsilon=0$ corresponding to the solution (4.14) with $v=+a$ when the minus sign chosen in Eq. (4.14) (first equation). Increasing ϵ appears to have a similar effect to that of introducing a phase shift to the solution. For $a=6$ and $b\geqslant 0$, it is clear from Fig. 4(b) that $a>a_c$ and so only two real constant equilibrium states are available.

2. Example 2: a=1

In this case the solution from Eq. (4.29) is

$$-\frac{1}{2}\ln\left[\tan\left(\frac{F}{4}\right)\right] - \frac{\epsilon}{512}\int^{F}\left[\cos\left(\frac{r}{4}\right)\right]^{-5/2}\left[\sin\left(\frac{r}{4}\right)\right]^{-7/2} \times\int_0^r\left[\tan\left(\frac{s}{4}\right)\right]^{1/2}\cos\left(\frac{s}{2}\right)dsdr = p. \tag{4.31}$$

Solutions for various values of ϵ are shown in Fig. 5(b). Similar to Fig. 5(a), as ϵ increases there also appears to be an effect comparable to a phase shift of the solution at $\epsilon=0$. It is also clear that these solutions are attempting to travel from a state larger than 2π to zero as p increases. Recall that $\phi(X,T)$ is equivalent to $(F(p)+\pi)/2$, by the relations (4.3) and (4.6) and therefore the solution ϕ is attempting to travel between states that differ slightly from the states $\pi/2$ and $\frac{3}{2}\pi$: this behavior can be anticipated by considering the qualitative features of a graph that will be similar in nature to that displayed in Fig. 3(a). Notice that $a<a_c$ when $a=1$ and $0\leqslant b\leqslant 0.0625$, as can be seen from Fig. 4(b), which indicates that four real constant equilibrium states are available.

These two examples above can further be interpreted in terms of the available equilibrium solutions in terms of ϕ as indicated in Fig. 6, which shows the dependence of the equilibrium states upon b for $a=1$ and $a=6$. For $a=6$ the equilibria for ϕ at $\pi/2$ and $\frac{3}{2}\pi$, available when $b=0$, both increase as b increases; for $a=1$ the equilibrium $\phi=\pi/2$ increases while $\phi=\frac{3}{2}\pi$ decreases as b increases above zero. Figure 6 should be compared with Fig. 4 where b, rather than a, was held fixed. There is a critical value $b_c=0.225$ when $a=1$ for which there are only ever two real equilibrium states for $b>b_c$: this should be compared with the result in Fig. 4(b). Consistent with the comments in the previous paragraph and the indications in Fig. 5, the equilibrium states between which the solutions travel are shifting slightly as b increases from zero.

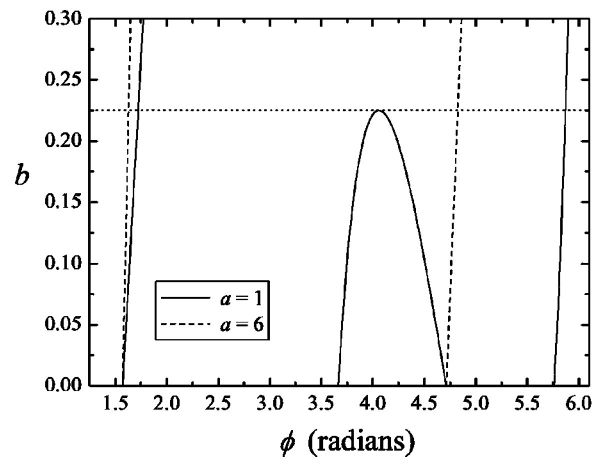

FIG. 6. Plots of the available constant equilibrium solutions ϕ for $a=6$ and $a=1$ corresponding to the examples in Eqs. (4.30) and (4.31), respectively: recall that $F(p)=2\phi-\pi$. There is a critical value $b_c=0.225$ when $a=1$ such that only two real equilibria occur for $b>b_c$ [cf. Fig. 4(a)].

V. DISCUSSION

An insight has been gained into solutions of the dynamic equation (2.11) for the orientation angle $\phi(x,t)$ of the vector **c** in SmC* liquid crystals under the application of an applied electric field. Knowledge of ϕ allows a complete description of the orientation of the usual liquid crystal director **n**, as discussed in Sec. II. In Sec. III possible equilibrium solutions for ϕ, between which traveling waves may occur, were identified and discussed in relation to the nondimensional control parameters a and b introduced via the relations (3.1) and (3.2); these parameters reflect the influence of the electric field contributions and tilt of the field, respectively. The identification of critical values a_c and b_c where the number of possible equilibria for ϕ changes from four to two as a or b increases were discussed in Secs. III and IV D, typical qualitative results being displayed in Figs. 4 and 6.

Lie point symmetries were investigated in Sec. IV, where solutions to a novel nonlinear approximation to the nondimensional form of the dynamic equation (2.11), given by Eq. (4.4), were considered. This analysis revealed the implicit solutions (4.29) for small values of b, obtained by considering a perturbation of the special case where $b=0$, when an exact traveling wave solution, given explicitly by Eq. (4.14), is available. The Lie point symmetries discussed in Sec. IV enabled the analysis of the governing partial differential equation to be reduced to that of an ordinary differential equation which was much more tractable both analytically and numerically. The point symmetries also revealed that $X+vT$ is the required invariant to use in order to make this reduction to an ordinary differential equation. Examples of implicit solutions [special cases of Eq. (4.29)] for $a=1$ and $a=6$ were discussed in Sec. IV D and plots of these solutions were given in Fig. 5 for various small values of b. Behavior similar to small phase shifts seems to occur in the numerical plots of these examples.

The stability properties for the traveling wave solutions derived here remain to be tackled. The case for $b=0$ can be handled by the methods employed in a similar problem for time-independent solutions discussed by Anderson and Stewart [21], which revealed the stability of nonconstant solutions $\phi(x)$ to an equation of the form (2.12); the stability of constant equilibrium states was also discussed by Anderson and Stewart [22] when $b=0$ (see also [23,24]). Such methods may yield information, via eigenvalue problems, on how the stability is influenced by the control parameters a and b through their contributions to the positivity of the first eigenvalue. Stability of the traveling wave solution (4.14) in the case when $b=0$ has been investigated by Stewart [14] (note that ϕ in [14] is equivalent to $\phi+\pi/2$ in the above and that the notation for the constant coefficients differs). Different types of behavior for small perturbations to the solution became evident via a spectral analysis which demonstrated that monotonic or oscillatory decay of perturbations may be combined with a phase shift to the original traveling wave solution, the possible occurrence of these phenomena being dependent upon, and selected by, a single nondimensional control parameter. It is anticipated that a similar spectral analysis may be feasible for the above implicit solutions when $b\neq 0$, and this is currently under investigation. The situation will be more complex than that discussed in [14] due to the presence of two control parameters rather than one.

ACKNOWLEDGMENT

E. M. acknowledges support from the National Research Foundation, South Africa, Grant No. 2053745.

APPENDIX

In this appendix we briefly summarize the main features of Lie point symmetries. The approach developed by Lie (see also Bluman and Kumei [25], Ibragimov [26,27], Olver [28], and Ovsiannikov [29]) gives a systematic way of determining infinitesimal point transformations

$$\overline{T}\approx T+a\xi^1(T,X,u),\ \overline{X}\approx X+a\xi^2(T,X,u),\qquad \overline{u}\approx u+a\eta(T,X,u), \tag{A1}$$

which leave Eq. (4.5) form invariant. The transformations (A1) form a group, where a is the group parameter, if the group properties hold. The Lie point symmetry generator of the group (A1) is given by

$$Z=\xi^1(T,X,u)\partial_T+\xi^2(T,X,u)\partial_X+\eta(T,X,u)\partial_u, \tag{A2}$$

where $\partial_T=\partial/\partial T,\ldots$, and

$$\xi^1(T,X,u)=\left.\frac{\partial\overline{T}}{\partial a}\right|_{a=0},\quad \xi^2(T,X,u)=\left.\frac{\partial\overline{X}}{\partial a}\right|_{a=0},\qquad \eta(T,X,u)=\left.\frac{\partial\overline{u}}{\partial a}\right|_{a=0}. \tag{A3}$$

The functions ξ^1, ξ^2 and, η are calculated by solving the determining equation found by acting the operator Z on Eq. (4.5) as indicated by

$$Z\left[u_T-u_{XX}+4a\sin\left(\frac{u}{2}\right)+4\sin u\right]\Bigg|_{(4.5)}=0. \tag{A4}$$

Equation (A4) is separated by coefficients of derivatives of u. The resulting system of linear equations can easily be solved. Equation (4.5) admits Lie point symmetries of the form

$$X_1=\partial_T,\ \ X_2=\partial_X. \tag{A5}$$

These Lie point symmetry generators can easily be found using computer algebra packages (see, e.g., Head [30], Sherring *et al.* [31], and Baumann [32]). The Lie point symmetry generators (A5) are indicative of Eq. (4.5) being autonomous. The Lie point symmetries (A5) can be used to show that Eq. (4.5) admits traveling wave solutions of the form

$$u(X,T)=F(p),\ \ p=X+vT. \tag{A6}$$

[1] *Solitons in Liquid Crystals*, edited by L. Lam and J. Prost (Springer-Verlag, New York, 1992).

[2] P. G. de Gennes and J. Prost, *The Physics of Liquid Crystals*, 2nd ed. (Clarendon, Oxford, 1993).

[3] S. T. Lagerwall, *Ferroelectric and Antiferroelectric Liquid Crystals* (Wiley-VCH, Weinheim, Germany, 1999).

[4] I. W. Stewart, *The Static and Dynamic Continuum Theory of Liquid Crystals* (Taylor and Francis, London and New York, 2004).

[5] N. A. Clark and S. T. Lagerwall, Appl. Phys. Lett. **36**, 899 (1980).

[6] I. Abdulhalim, G. Moddel, and N. A. Clark, Appl. Phys. Lett. **60**, 551 (1992).

[7] I. Abdulhalim, G. Moddel, and N. A. Clark, J. Appl. Phys. **76**, 820 (1994).

[8] J. E. Maclennan, Qi Jiang, and N. A. Clark, Phys. Rev. E **52**, 3904 (1995).

[9] P. Schiller, G. Pelzl, and D. Demus, Liq. Cryst. **2**, 21 (1987).

[10] P. E. Cladis and W. van Saarloos, in *Solitons in Liquid Crystals* (Ref. [1]), pp. 110–150.

[11] J. E. Maclennan, N. A. Clark, and M. A. Handschy, in *Solitons in Liquid Crystals* (Ref. [1]), pp. 151–190.

[12] W. van Saarloos, M. van Hecke, and R. Holyst, Phys. Rev. E **52**, 1773 (1995).

[13] I. W. Stewart, IMA J. Appl. Math. **61**, 47 (1998).

[14] I. W. Stewart, Phys. Rev. E **57**, 5626 (1998).

[15] F. M. Leslie, I. W. Stewart, and M. Nakagawa, Mol. Cryst. Liq. Cryst. **198**, 443 (1991).

[16] F. M. Leslie, I. W. Stewart, T. Carlsson, and M. Nakagawa, Continuum Mech. Thermodyn. **3**, 237 (1991).

[17] T. Carlsson, I. W. Stewart, and F. M. Leslie, J. Phys. A **25**, 2371 (1992).

[18] F. M. Leslie, in *Advances in the Flow and Rheology of Non-Newtonian Fluids, Part A*, edited by D. A. Siginer, D. De Kee, and R. P. Chhabra (Elsevier, Amsterdam, 1999), pp. 591–611.

[19] I. W. Stewart, T. Carlsson, and F. M. Leslie, Phys. Rev. E **49**, 2130 (1994).

[20] A. D. Polyanin and V. F. Zaitsev, *Exact Solutions for Ordinary Differential Equations* (CRC Press, Boca Raton, 1995).

[21] D. A. Anderson and I. W. Stewart, Int. J. Eng. Sci. **39**, 1191 (2001).

[22] D. A. Anderson and I. W. Stewart, Phys. Rev. E **62**, 5043 (2000).

[23] T. Carlsson, I. W. Stewart, and F. M. Leslie, Liq. Cryst. **9**, 661 (1991).

[24] M. Nakagawa, J. Phys. Soc. Jpn. **59**, 81 (1990).

[25] G. W. Bluman and S. Kumei, *Symmetries and Differential Equations* (Springer-Verlag, New York, 1989).

[26] N. H. Ibragimov, *CRC Handbook of Lie Group Analysis of Differential Equations Vol. 1* (CRC Press Inc., Boca Raton, FL, 1994).

[27] N. H. Ibragimov, *Elementary Lie Group Analysis and Ordinary Differential Equations* (J. Wiley and Sons, Chichester, 1999).

[28] P. J. Olver, *Applications of Lie Groups to Differential Equations* (Springer-Verlag, New York, 1986).

[29] L. V. Ovsiannikov, *Group Analysis of Differential Equations* (Academic, New York, 1982).

[30] A. K. Head, Comput. Phys. Commun. **77**, 241 (1993).

[31] J. Sherring, A. K. Head, and G. E. Prince, Math. Comput. Modell. **25**, 153 (1997).

[32] G. Baumann, *Symmetry Analysis of Differential Equations With Mathematica* (Springer-Verlag, Berlin, 2000).